UNDERGRADUATE DISSERTATION

Supported membranes development for methanol synthesis reactors

Author:
Ester Juárez Rodríguez

Supervisor:
Miguel Menéndez Sastre

A dissertation submitted in fulfillment of the requirements for the degree of Biotechnology

in the

Chemical Engineering and Environmental technologies Department
Sciences Faculty
Engineering Research Institute of Aragon (I3A)

June 26, 2021

Contents

List of Figures

List of Tables

List of Symbols

Appendix C.1. Flows and models

$\overline{x}_i$	Mean volumes	mL
t	Time	s
p	Pressure	atm
$R = 0.082$	Molar gas constant	$\frac{L*atm}{K*mol}$
T	Temperature	K
p^*	Overpressure	Pa
$\pi = 3.14$	Pi constant	-
$r = 0.0034$	Inner radius of the ceramic support	m
$h = 0.052$	Length of the ceramic support	m
ϵ	Porosity	-
r_{pore}	Pore radius	m
L	Pore length	-
$\tau =$??	Tortuosity	-
$M = 0.028$	N_2 Molecular mass	kg

Appendix C.2. Calculated parameters

$\chi_{perm,a}$	Molar fraction of a in the retentate	-
$\chi_{a,in}^{perm}$	Input molar fraction of a in the permeate stream	-
ΔP_a	Difference of logarithmic mean pressure of a	bar

Acknowledgements

I would like to thank Miguel and all the people from the lab, specially Javier, for being so patient with my repetitive mistakes. Your great mood leads to greater work.

Guillermo, you could see a biotech in me even before I knew it. I could not have dreamed for better support over these years. I am willing to dedicate many more projects to you.

Abstract

Methanol can be obtained by CO_2 hydrogenation in a membrane reactor with higher yield or lower pressure than in a conventional packed bed reactor. This work explores a new kind of membrane with the potential to be suitable for such membrane reactor. Silicone-ceramic composite membranes and Nafion® have been synthesized and characterised towards the capability to selectively remove H_2O from a mixture containing H_2, CO_2 and H_2O at adecuate temperatures for methanol synthesis. We have found that silicone membranes can provide selective permeation of H_2O under such harsh conditions, and thus is an alternative candidate for its use in membrane reactors for this process.

Chapter 1

Introduction

1.1 Environmental context

The current world energy system is based on fossil fuels [1] [2]. It is well known that fossil fuels based industry promotes greenhouse emissions [3], which ultimately have a strong negative impact on the environment. As world population rises, also do energy demands over these energy sources. Although there are still many oil and natural gas reserves, it is getting ever harder to access them as they are located in remote places like Siberia or Antarctica. Thus, clean energy alternatives are often needed.
Besides being environmentally friendly, such alternatives will be needed in the future of our society. They must be financially feasible, continuous all year, safe and easy to carry and store, among other requirements. Wind and solar energy have so far demonstrated to be the best approaches for this great challenge. However, both of them have major drawbacks: they are intermittent with excess energy production in short periods of time, need new infrastructure and their yield varies on different locations.
For the future development of clean energies, it has been proposed the exploitation of methanol industry, for it has a number of advantages compared to hydrogen as an energy carrier [4]. Both of them are simple molecules that store electrons, but there are technical implications in the processes of obtaining them. For instance, methanol can be obtained by the reduction of CO_2, making it a neutral carbon fuel. It is less volatile than hydrogen and has higher volumetric density, making storage and transportation safer. In addition, it is relatively easy to take advantage of oil infrastructure [5].

1.2 Methanol economy and state of the art

Methanol is a core commodity in the chemical industry. Biomass, natural gas, coal, oil, renewable energies, atmospheric CO_2 are some of the feed stock sources available to obtain it. Later it would be raw material for many important compounds in the chemical industry like acetic acid, gasoline, olefines, propylene or formaldehyde. Methanol is therefore well-established in the chemical industry of construction, electronics, appliances, pharmacy, plastics and many others. [6]

There have been attempts in the past of building a methanol based energy industry. For example, it was used as transportation fuel in California for a few decades and was a main source of gasoline production in New Zealand [7]. Nowadays, there are multiple international cooperative projects and companies looking for a financially suitable solution [8]. Appendix A provides a list of European-funded research projects. A company in Iceland has developed a process of methanol synthesis from geothermal CO_2 emissions [9].

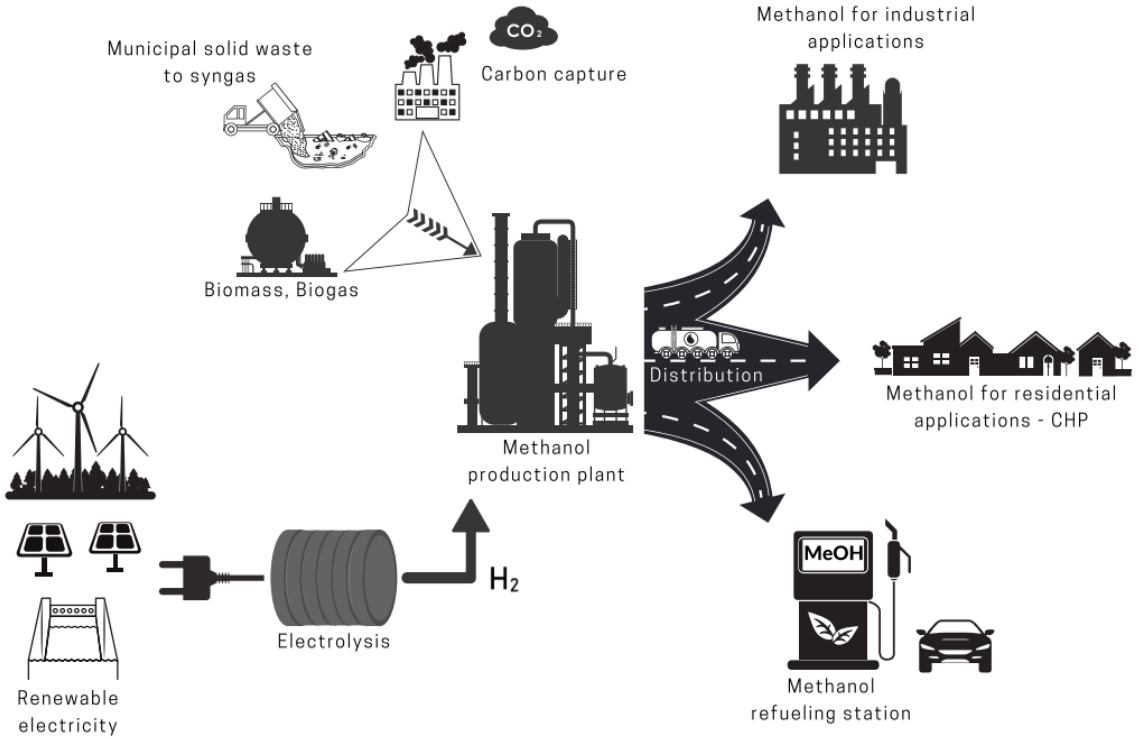

Figure 1.1: Methanol economy. Image provided by Araya et al [6] under an open access Creative Common CC BY license.

While oil has been a though competitor over the last decades, methanol has not been employed as an energy vector, mainly because there are still setbacks on its production. Hydrogen cost, if obtained by water electrolysis is too high. Only with further decreases in the electricity and electrolizer cost and increases in oil prizes, green methanol cost will compete with fossil fuels. A problem that increases the production cost are the soaring pressures of 50-100bar to achieve suitable yield at the reactor exit. This project focuses on methanol synthesis by hydrogenation of syngas mixtures with CO_2 and H_2, that has proven to be a scalable strategy [5]. CO_2 from antropogenic emissions would be fixed back to a hydrocarbon fuel molecule, closing the loop. Due to the thermodynamic limitations in the maximum achievable yield in reaction 1.1, which is also lowered by competitive reaction 1.2, this process is subject to process intensification.

$$CO_2 + 3H_2 \Longleftrightarrow CH_3OH + H_2O, \quad -49.51kJ/mol \tag{1.1}$$

$$CO_2 + H_2 \Longleftrightarrow CO + H_2O, \quad 41.19kJ/mol \tag{1.2}$$

$$CO + 2H_2 \Longleftrightarrow CH_3OH, \quad -90.70kJ/mol \tag{1.3}$$

Process intensification consists in the development of improvements in existing chemical manufacturing processes that provide drastic reduction in capital, operating costs or in environmental impact. It usually combines two or more steps of a large process into a single device. Reactive separations are one of the most popular strides [10], as the traditional distillation processes are quite energy intensive.

It has been demonstrated in many experiments that reaction 1.1 is predominant in the mechanism of industrial methanol synthesis. Being an exothermic reaction, methanol formation is favored by lower temperatures and high pressure. However, methanol industrial synthesis peaks at temperatures lower than 250ºC, diverting the mechanism towards the competitive reaction 1.2.
Both high pressure and high temperature are economical and technical challenges in this process. Thermodynamic and kinetic limitations are key concerns over yield methanol production. A compromise has to be achieved between CO_2 conversion and cost of commissioning of pressure and temperature conditions.

1.3 Membrane reactors

Membrane reactors have been proposed to remedy said predicament. The premise is to develop a bi-functional reactor that catalyses the conversion of CO_2 into methanol and separates the products with a selective membrane. By the Le Châtelier principle, such separation would shift the reaction 1.1 equilibrium to methanol formation, on adequate conditions. If there is better conversion of CO_2 and yield, less demanding conditions of pressure and temperature will be needed, making the process more feasible.
Although this dissertation revolves around membrane development, catalysts are very important elements in this technology. Due to its high thermodynamic stability ($\Delta G = -394.38 kJ/mol$) and kinetic inertness, CO_2 is not easy to activate, and a catalyst is needed. $Cu - ZnO$ heterogeneous catalysts are the most studied ones in the process of CO_2 hydrogenation from syngas, but noble metals like Pd and Au are being taken into consideration too. Research in this field is targeted at understanding the molecule mechanism of the catalysts that showed better results and preventing their inactivation at high temperatures and humidity [11].
Several researchers have attempted to use a membrane reactor to increase the yield in methanol synthesis. In 1995, Struis et al [12] were pioneers in achieving better methanol conversion using Nafion ® membranes. Barbieri et al [13] have developed a mathematical model of membrane reactor, showing the improvements that can be achieved. Liu et al [14] have propose a composite polymer/ceramic membrane to be used in pervaporation.
The Chemical Engineering and Environmental technologies Department of the University of Zaragoza also has a remarkable know-how in membrane reactors technology. By 2003, Menéndez et al had already patented a zeolite membrane reactor for methanol synthesis [15], which was successfully validated by Galluci et al [16].

1.4 Flow models through membranes

Membranes in the reactor have two roles: one is to extract H_2O and/or methanol from the place where the reaction is being held, and the second is to not let CO_2 and H_2 out. In other words, membranes have to be selective to H_2O and methanol, stable at relatively high temperatures (close to 200ºC), structurally resistant and without defects. With all reactants and products being in gas state at 200ºC, two types of selective flows might be taking place: capillary condensation or solution-diffusion mechanism.

If the membrane is porous, the most accepted selective flow model is capillary condensation. In this mechanism, increased Van der Waals interactions inside the pores cause condensation of the molecules at partial pressures below their saturation vapor pressure. During CO_2 hydrogenation, methanol and water condensation in the membrane pores may block the flow of non-condensable gases and dissolve into it. Channels [17] inside the membrane allow the two compounds to travel to the other side of the membrane with the driving force of a difference in partial pressure. Water and methanol soak the membrane, not letting CO_2 and H_2 follow the same route at the same rate. The final result is a separation between the products of the reaction and the reactants and improving CO_2 conversion.
If the membrane is non-porous, solution-diffusion flow model is more accepted. Gas molecules will dissolve on the upstream surface of the membrane, diffuse across the membrane and desorb on the downstream face of the membrane. Mass transport will be mainly controlled by diffusion coefficients and concentration gradients.
In addition to the above described mechanisms for selective flow, tow mechanism for non-selective flow may occur in porous membranes: laminar flow and Knudsen flow. Pore size determines how molecules diffuse through the membrane. If the pore diameter is small enough, molecule interactions will be more predominant with the membrane walls than with other molecules. Diffusion over the membrane will therefore be governed by a Knudsen type diffusion [18]. If the pores are not so small, flow through them will be laminar. The equations for laminar and Knudsen flow are described in Appendix C.

1.5 Membrane choices

During the first experimental results, membrane damage and inactivation were major problems. For that reason, a resistance model for composite membranes has been the ongoing approach. This type of membranes have a layer of a mechanically and heat resistant ceramic material that acts as support and a top thinner coating layer of a polymer [19]. The thin layer contributes to selectivity while the ceramic layer provides mechanical resistance. The resulting supported membrane will be more stable and functional in operating conditions.
Different protocols on composite membrane preparation lead to a variety of results in the permeation experiments [20]. The modelling of how these membranes work at molecular level are still in progress, as they are complex structures with often dynamic pores. Because of that, trial-and-error is a practical strategy for developing supported membranes for methanol synthesis reactors.

Finally, membrane choice must be economical and scalable. Taking all of these factors into account, zeolite membranes have shown fantastic separation factors, with a remarkable decrease in temperatures close to 240ºC. [21] [22]. Silicone rubber and Nafion ® (sulfonated tetrafluoroethylene based fluoropolymer-copolymer) polymers have also prove to be viable options coating ceramic membranes [23] [24] [25] [26]. In this line, silicone and Nafion ® protocols for membrane preparation have been studied in this project.

1.6 Objectives

There are three consecutive objectives in this project:

* Analysis of heat resistant polymers that are potentially selective to water.
* Development of new protocols for the preparation of supported membranes of the chosen polymers.
* Permselectivity assays in several conditions of water partial pressure and temperature, using reactants concentrations that simulate real feed flow.

Chapter 2

Experimental design and methodology

2.1 Supported membranes preparation

Both polymers were meant to be deposited as a thin uniform layer over the ceramic membrane. However, silicone and Nafion® presented different challenges for the preparation protocols. Although this chapter discusses the methodology used in membrane characterization, many details have been developed in a significant part of the experimental phase of this project.

2.1.1 Silicone membranes preparation

Silicone was purchased as non-polymerized mid-range room temperature vulcanized (RTV-801) cristobalite, together with the catalyst dibutyltin dilaurate (abbreviated DBTDL).
Different temperature ramps from 25ºC to 250ºC were tested in order to check that the silicone could endure methanol synthesis reaction temperatures. There were no visible changes in the membranes with increased ramp slopes.
After following the polymerization process recommended by the manufacturer, the silicone was not thin enough. It was necessary to find a solvent that did not interfere with the polymerization process and evaporated right after, so it would not add thickness to the membrane.
As silicone is hydrophobic, organic solvents were expected to be more efficient at dissolving it. Still, some hydrophilic and acidic solvents were put into test: water, alcohol, acetone, ethanol, nitric acid, ortophosphoric acid and sulphuric acid. Hydrophilic solvents did not dissolve silicone significantly, while strong acids negatively affected its integrity and therefore polymerization. Toluene and fractional hexane ($d_{hex} = 0.672 g/ml$) could dissolve the silicone, but only fractional hexane evaporated without damaging the polymer.
Although membranes preparation protocol development was based on Chen et al work [23], catalyst proportion, heat fixation and layering were some of the few factors that were worth to take into consideration. Finally, the protocol consisted in a solution casting of the already polymerized silicone dissolved in fractional hexane. Membrane calcination changed its properties, making it an optional step. Layering is as simple as repeating the solution casting steps, as new silicone layers do not elute the previous ones. The weight of the new multi-layered membrane is expected to be proportional to the total silicone added. Step by step process is explained in more detail in Appendix B.

2.1.2 Nafion® membranes preparation

Nafion® is the brand name for a sulfonated tetrafluoroethylene based fluoropolymer-copolymer. It was purchased in two different formats: one as a 10%(w/w) aqueous solution (Ref: 527106-25ML Sigma Aldrich) and other as Nafion®-117 at 5%(w/w) alcohol solution (Ref: 70160-25ML Sigma Aldrich).

Even though some experiments have proved that interval heat activation and acid/base neutralization treatment improve Nafion® membrane properties [24] [25], this was not the case for our supported membranes. Previously documented protocols damaged the ceramic membrane and resulted in an irregular defective Nafion® layer.
Layering and heating were tested as well. Both alcohol and aqueous Nafion® solutions layers were thinner than the silicone ones. However, layering resulted in elution of the already deposited membrane. Calcination was not considered because Nafion starts to degrade at 200ºC. Heating up to 80ºC already showed damage in the membranes as they shed in scales.
Finally, the protocol applied was a simple inner coating of the ceramic membrane with the commercial Nafion® solutions: starting with a calcined enamelled ceramic membrane, which weight is known, pipette a known volume of polymer solution several times until it has fully covered the inner wall of the ceramic. Try to avoid bubble formation as it leads to irregularities on the membrane surface. Let it dry at room temperature and weigh again.

2.2 Membrane characterization: SEM and FESEM

Field emission scanning electron microscopy (FESEM) with Carl Zeiss: MERLIN^{TM} microscope and SEM with JEOL JSM 6400 of a few selected membranes provided valuable information about their thickness, integrity and surface. For it is a destructive analysis, the membranes photographed were no further characterised. They were representative samples of each membrane preparation protocol. Combining the results with previous weighing and inner surface measurements, this technique provided a method to calculate the density of the membranes.

2.3 Preliminary permeance experiments

Before testing the supported membranes inside the reactor with the reactant gases at high temperatures, pressurized air permeance was tested at room temperature as shown in Figure 2.1. Several variables were iterated in said provisional system throughout the membranes protocols development, such as the influence of enamelling, calcination, hexane treatment and catalyst concentration.

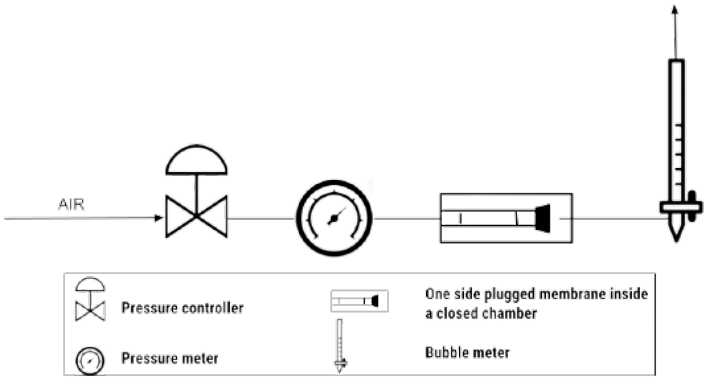

Figure 2.1: Flow diagram for preliminary air permeance measurements.

Time and volume measurements in the bubble meter, alongside environmental temperature and pressure led to an early approximation of the pore size of each membrane. All formulas used to follow the data flow shown in Figure 2.2 are in Appendix C.

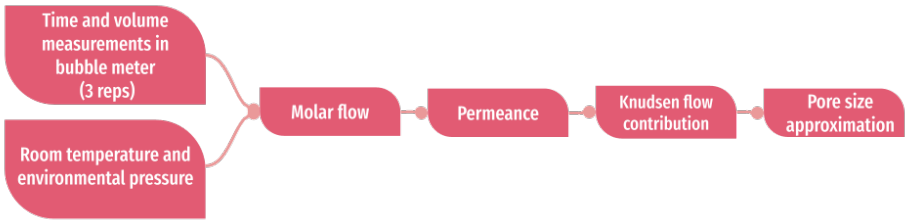

Figure 2.2: Schematic data flow for pore size approximation calculations.

As mentioned before in Chapter 1.4, small pore size favours Knudsen flow, potentially increasing H_2O/H_2 and H_2O/CO_2 selectivity in the membrane. Experimentally, data is collected as shown in Figure 2.3, and then Knudsen and laminar flows are calculated through a linear regression of the data set.

Before starting gas separation assays with the reactants, a few permeance measurements were ran over a membrane that was fitted inside the reactor. A known overpressure of N_2 or H_2 at different temperatures was applied to the membrane reactor. Although such experiments still provided information about convective flow through the membrane, they were useful when compared to the preliminary air permeance measurements.

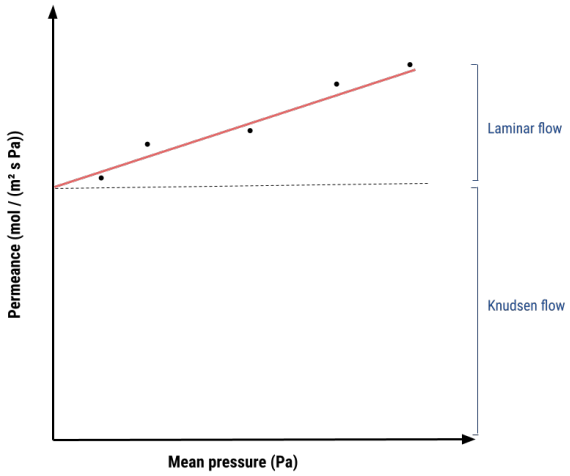

Figure 2.3: Linearization of empirical permeance results over mean pressure makes it possible to estimate the membrane pore size.

2.4 Gas separation assays

The last membrane characterization consisted in parallel feeding the reactor H_2, $H_2O(g)$, CO_2 and N_2 inside the membrane and Ar as dry sweeping gas outside the membrane at different controlled conditions (See Table 2.1). This difference in gas composition inside and outside the membrane did provide information about diffusive flow through the membrane, being material flow the driving force.

Temperature at constant $P_{H_2O} = 9.9kPa$		
180ºC	200ºC	220ºC
P_{H_2O} (kPa) at T=200°C		
5.2	9.9	18.0

Table 2.1: Different conditions tested for gas separation.

Even though these membranes are being developed for methanol synthesis, the following gas separation assays will not hold the chemical reactions involved in methanol synthesis with a significant yield because there is no catalyst present. Other projects revolving this subject that used similar conditions and a catalyst in the same lab facilities could detect traces of methanol in both the retentate and permeate products [21].
The quantities and proportions of each gas are represented in Table 2.2. CO_2 and H_2 are fed in the 3:1 stoichiometric proportion that is intended to favour reaction 1.1 at temperatures around 200ºC and low pressure.
In this modelled reaction, H_2O will serve as a marker of the membrane selectivity to the products (molecular diameters of CH_3OH and H_2O are in the same order of magnitude). Hence, N_2 and Ar are needed to act as dry inert sweeping gases in retentate and permeate, respectively. The purpose of testing different H_2O flows is to elucidate the pattern of selectivity of the membranes as the reaction yield increases. It could be linear or parabolic or rise until certain proportions and then plummet, providing information about the integrity of the membranes and the predominant flow that is taking place.

Compound	$H_2O(g)$	H_2	CO_2	N_2	Ar
STP Feeding stream (cm^3/min) at T=200°C	6.9	75	25	25	100
	3.7	75	25	25	100
	27.4	75	25	25	100

Table 2.2: Volumetric flows of the retentate (white cells) and permeate (gray cells) used in the experiments at standard pressure and temperature, before calibration.

The reactor that contained the membrane had four outlets: two of them were the entrance and exit of the retentate streamline and the other two had the same function for the permeate streamline. A small scale industrial plant was designed to carry both lines in parallel continuous flow (See Figure 2.4). H_2, CO_2 and N_2 were pumped from commercial bottled mixtures while liquid H_2O was vaporized and pumped with an HPLC pump (Shimadzu LC-10AT). Those four compounds entered the reactor and travelled inside the membrane as the input retentate streamline.

At the same time, Ar was pumped from a commercial bottle and introduced in the reactor to cover the outside of the membrane and carry the output permeate streamline. Temperature at the oven was automatically adjusted and controlled with a thermocouple system.
Assuming quick equilibrium of each compound is achieved during the experiment on both compartments of the reactor, outlet permeate and retentate streamlines compositions should be representative of H_2O/H_2 and H_2O/CO_2 selectivities and separation factors, among others.

Output H_2O vapor will be quantified as weight added in cold traps and the rest of the gases will enter the gas chromatograph (SRA Instruments MicroGC R3000) attached to the circuit. Excepting Ar, every compound had to be previously calibrated in the gas chromatograph. The results obtained with the proprietary software (See Figure 2.5) could be exported as `.pdf` format and later processed. Because of the slow condensation of the outlet vapor and the need of accuracy in every sample, each test condition lasted at least two hours with retentate and permeate analysis interspersed two and even three times. A 3-way ball valve allowed to divert both streamlines and measure their volumetric flows with a bubble meter.

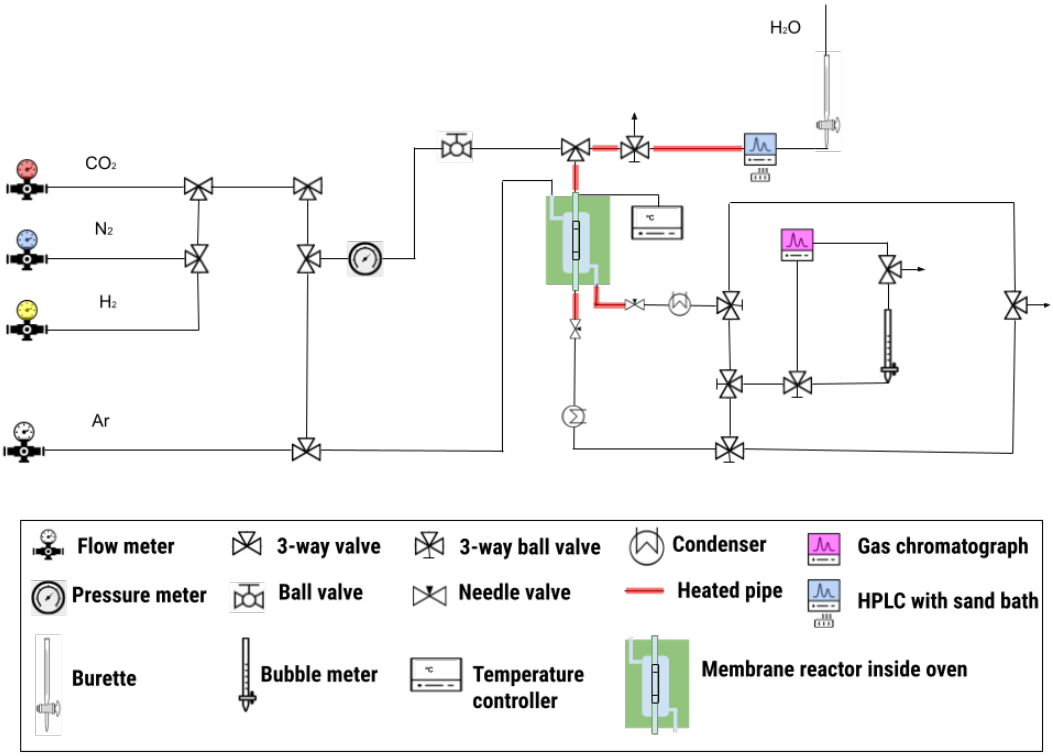

Figure 2.4: Schematic small scale industrial plant for gas separation assays.

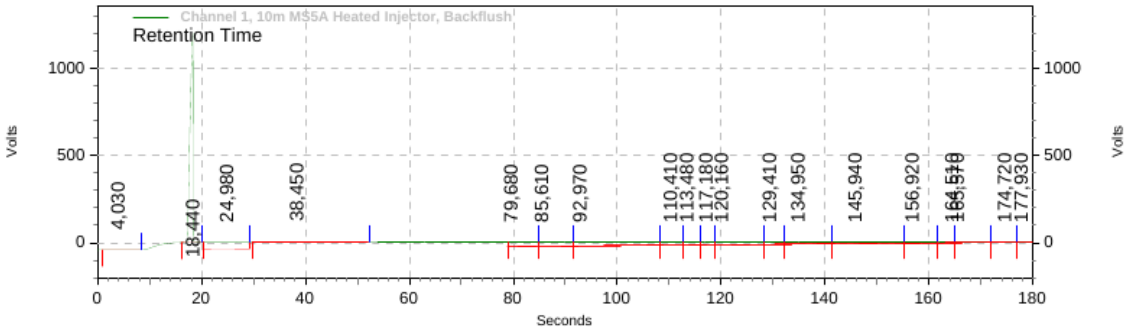

Figure 2.5: Example of a gas separation result.

Finally, fitting the membrane inside the reactor required covering part of it with lubricant and graphite and sealing it by applying a considerable shear stress. There was a significant risk in damaging the membrane or even breaking it in the assembling process.

Chapter 3

Results and discussion

3.1 Preliminary permeance experiments

N_2 permeance in ceramic membranes was tested at room temperature before applying polymer membranes and showed consistent results in the lower range of $10^{-5} \frac{mol}{m^2 sPa}$.
Enamelling and calcination did not change those results, and either did treatments with fractional hexane and/or DBTL catalyst. However, after leaving a sample of ceramic membrane submerged in DBTL overnight, it gained some weight, suggesting that the catalyst does not dissolve the membrane but interacts with its surface and gets absorbed in some concentration dependent degree.

3.1.1 Silicone and Nafion® membranes: Knudsen contribution and pore size estimation

The next step was to measure air permeance at room temperature through the membranes as Chapter 2.3 explained. Knudsen flow contribution and pore size were roughly estimated through linearization of the results (Figure 2.3). However, these experiments only served as practical screening methods for the membranes because the conditions set were not similar to the gas separation assays. The premise was that membranes with higher Knudsen contribution had smaller pore size. In tables 3.1 and 3.2, membrane preparation protocols are compared in order to find out which produced higher Knudsen contributions. Some protocols were replicated because they tended to generate inconsistent results (e.g. T4 and T5) or one of the replicates would be sent to FESEM analysis and therefore destroyed.
It is important to mention that standard deviations have not been represented because many membranes did not change their permeance values as the mean pressure raised. Linearization of this results almost had no slope, hence every minimal deviation would produce disproportional and non representative standard deviations.

Overall, silicone membranes showed higher Knudsen contributions compared to the Nafion® membranes, ranging from 34.6% to 99.9%. Nafion® membranes did not exceed 38.9% Knudsen contribution. Heavy silicone membranes preparation protocol suggested to be the most effective in generating smaller pore sizes. Calcination step did not apparently produce any effect on the permeation results, yet this conclusion should be more thoroughly tested.

ID	Preparation protocol	Calcination	Layers (wt%)	% Knudsen
T1	**Heavy**	No	5 + 5	93.6%
T2	**Heavy**	No	5 + 10	99.9%
T3	**Heavy**	No	10	99.9%
T4	**Heavy**	Yes	7.5	86.8%
T5	**Heavy**	Yes	7.5	46.0%
T7	**Heavy**	No	7.5	83.6%
T8	**Heavy**	No	7.5 + 2.5	34.6%
T9	**Light**	No	7.5	83.1%
T13	**Heavy**	No	7.5 + 2.5	63.6%

Table 3.1: Silicone membranes preparation protocols against Knudsen contribution. Pink: membranes that were measured later in gas separation assays. Blue: membranes that were analysed with FESEM and SEM.

Layering produced opposite effects depending on the polymer used. In silicone membranes, more total layer weight led to less permeance and generally higher Knudsen contribution, regardless of the order each layer was applied. Conversely, Knudsen contribution of Nafion® membranes decreased as more layers were applied.
It should be noted that preparing these membranes was a simple but challenging protocol. One of the innovative aspects of this project was to manufacture Nafion® membranes on ceramic supports instead of buying commercial self-supported membranes, like it has already been done by Ren et al [24], Siroma et al [25] and other research teams. Due to its delicate nature, it was convenient to buy the polymer already dissolved in two different solutions (alcohol and aqueous).

Those solutions had three important drawbacks. Firstly, bubbles formed very easily during the inner coating of the membranes, leading to an uneven surface. Secondly, each layer dissolved and dragged the previous one, which was a hinder when determining the actual Nafion® that deposited on the support. Thirdly, the polymer was sensible to heat in both aqueous and alcoholic solutions, so trying to increase its concentration by evaporation of the solvent instead of layering was not effective.

ID	Preparation protocol	Layers (wt%)	% Knudsen
T10	**Inner coating**	10 + 10 + 10 (aq)	26.3%
T11	**Acid/base neutralization**	5 (alcohol)	0%
T12	**Inner coating**	10 + 10 (aq)	0%
T14	**Inner coating**	10 (aq)	38.9%
T15	**Inner coating**	10 (aq) + 5 (alcohol)	3.5%

Table 3.2: Nafion® membranes preparation protocols against Knudsen contribution. Pink: membranes that were measured later in gas separation assays. Blue: membranes that were analysed with FESEM and SEM.

After experimenting with different techniques in the development of the Nafion® membranes preparation protocols, a single inner coating of the 10% (w/w) aqueous solution resulted in a higher

Knudsen contribution. Furthermore, acid/base neutralization significantly damaged the membranes and led to higher permeance with predominant laminar flow.
As a final preliminary experiment, T5 was later placed inside the reactor and N_2 and H_2 permeances were measured separately at different pressures and temperatures as it is shown in Figures 3.1 and 3.2. The purpose of this intermediate step was to confirm whether the silicone membranes could endure reaction temperatures.

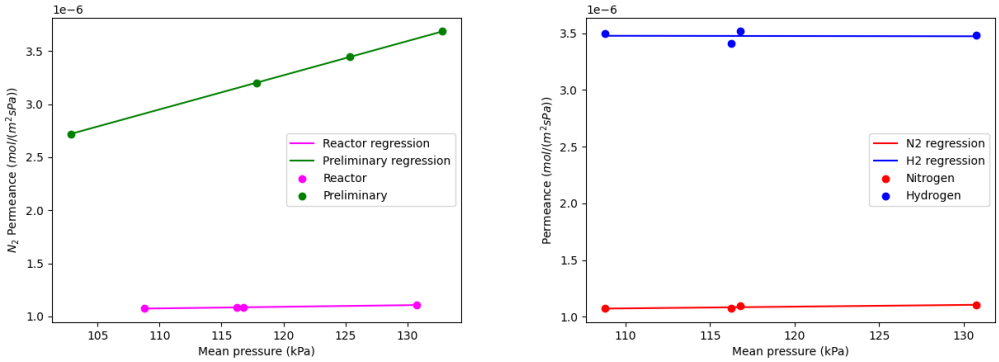

Figure 3.1: Experiments at room temperature. Left: N_2 permeance through the preliminary permeation installation and inside the reactor; Right: Difference between H_2 and N_2 permeances with T5 inside the reactor.

The plot on the left in Figure 3.1 represents how N_2 permeance is significantly reduced when T5 is placed inside the reactor. Being H_2 a smaller molecule than N_2, higher H_2 permeance is expected with Knudsen flow. On the right, a higher H_2 permeance alongside a discreet slope in the linear regression suggests that Knudsen flow is predominant inside the reactor.

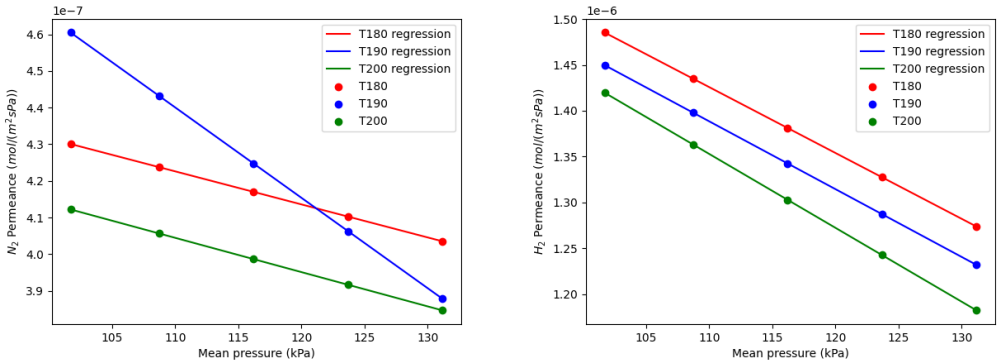

Figure 3.2: Left: N_2 permeance experiments near reaction temperature; Right: H_2 permeance experiments near reaction temperature;

Figure 3.2 represents similar decreasing patterns in gas permeances as temperature increases. Again, H_2 has a greater permeance, in this case even in a whole order of magnitude. Such descent

might be caused by the narrowing of the kinetic membrane pores because of the temperature elevation. Other possibility could be that the polymer swells at high temperatures. Either way, the silicone membrane presumably endured such temperatures.
With this intermediate experiments, pore sizes estimations should be closer to their real values, as the placement in the reactor provides a more reliable setup. Table 3.3 displays the pore size estimations of every membrane that was later measured on gas separation assays. Again, high Knudsen contributions produce enormous standard deviations. They are not represented because this table is just an approximation made from a suboptimal method.

ID	Pore radius estimation (nm)
T5	**93.8**
T10	**56.7**
T9	**89.6**
T15	**186**
T1	**54.9**

Table 3.3: Pore radius estimations calculated from N_2 permeance at room temperature of each membrane that was placed inside the reactor (in order). White: silicone membranes; Gray: Nafion® membranes

The criteria used for selecting which membranes would be tested in gas separation assays changed throughout the project. At the beginning, mediocre and disposable membranes were chosen because they would probably be damaged in the initial assays. Measuring their selectivity and permeance helped to pitch the ranges of several variables over the following experiments. Once the calibration and methodology were improved, some membranes with representative preparation protocols for each polymer were characterised both in FESEM/SEM and gas separation assays.

3.2 FESEM and SEM: membrane densities and evenness

FESEM results provided a superficial overview of the effects of different membrane preparation protocols. In Figure 3.3, the surfaces of silicone membranes (T4 and T8) are smoother than the Nafion® ones, which suggests that Nafion® are more irregular and uneven.
T4 membrane shows that there still are scales even after fractional hexane treatment posterior to calcination. The double silicone layer applied in T8 membrane can not be appreciated with this technique. Its plasticity and elasticity causes an irregular sectional pattern.
When taking a closer look at the supports of T11 and T12, some darker shadows indicate that both Nafion® preparation protocols (acid/base neutralization and inner coating) are harmful to the support. This is an important aspect to consider as any damage in the support will most likely produce larger pore sizes.

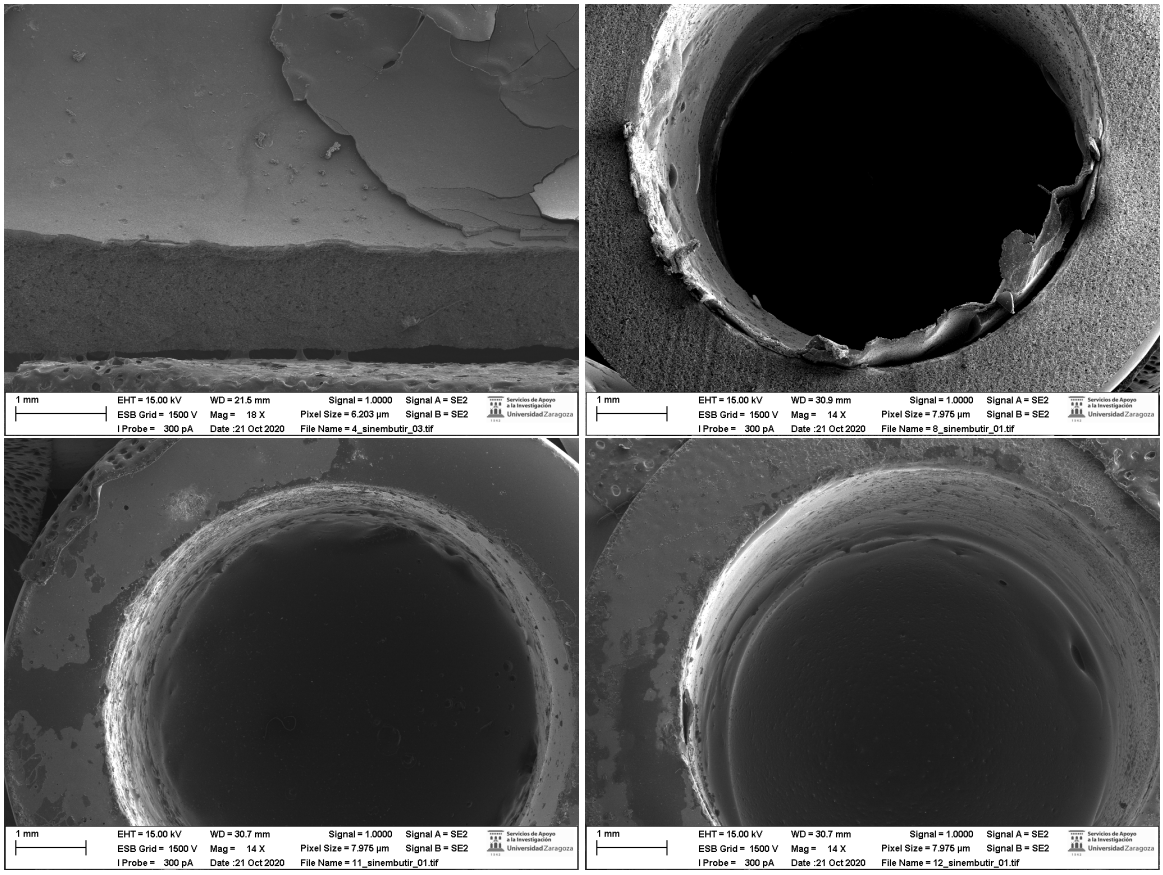

Figure 3.3: FESEM results. Upper left: T4; Upper right: T8; Bottom left: T11; Bottom right: T12.

SEM results allow to make a graphic calculation of each membrane density, as mentioned in Chapter 2.2. In Figure 3.4, silicone membranes revealed a continuous surface with a thickness around 75μm deposited on the ceramic support in the case of a single layer membrane (T4) and around 100μm for the double layer membrane (T8).
The thickness observed by SEM matches with the weight increase observed after membrane preparation (0.01 g/cm^2 in first case and 0.012 g/cm^2 in the second). In fact, the layer thickness estimated from weight increase (with a density of the polymer close to 1 g/cm^3) is a bit larger than the one measured by SEM, suggesting that some silicone has penetrated in the ceramic pores. In both cases, a quite continuous polymer layer was deposited on the ceramic support.

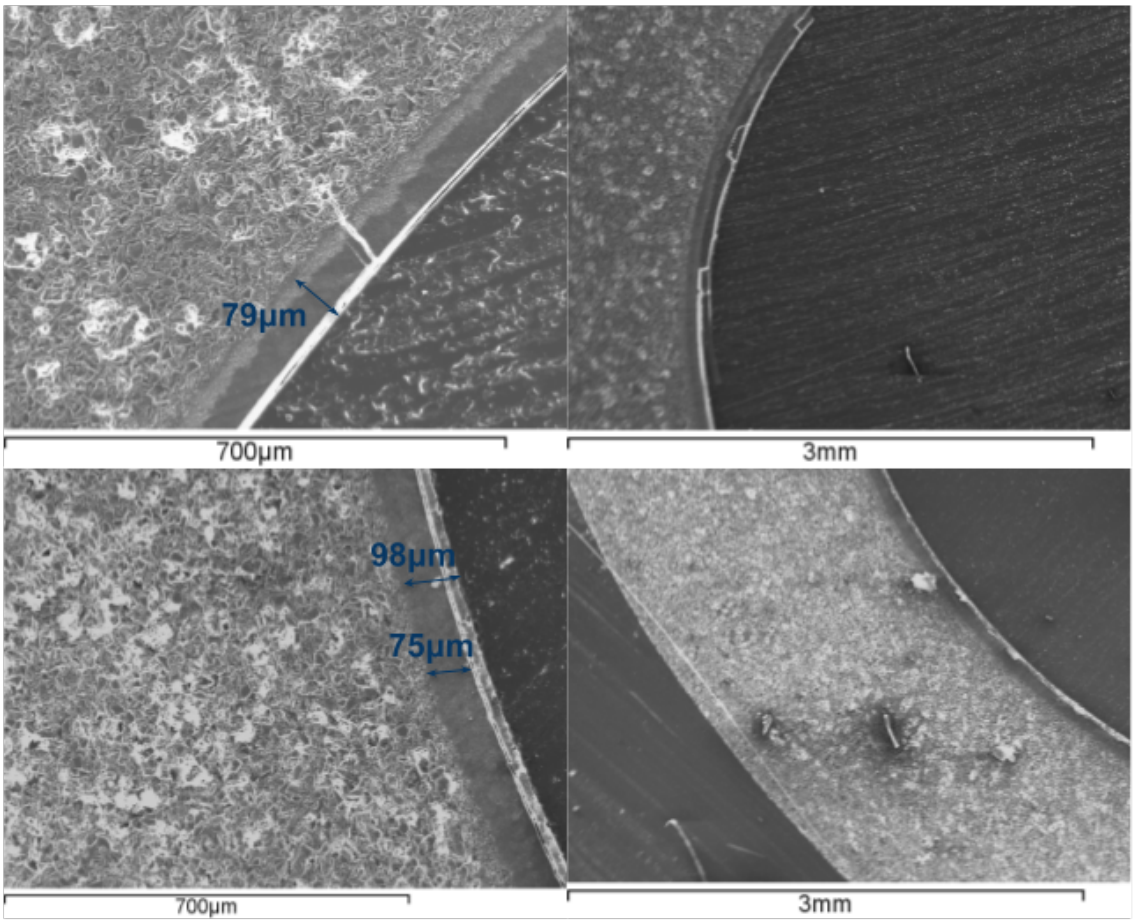

Figure 3.4: SEM results for silicone membranes. Upper row: T4; Bottom row: T8.

On the contrary, Nafion® prepared membrane with acid/base protocol (T11) exhibits severe irregularities in Figure 3.5 throughout all its surface. A rough estimation of its density from weight increase (1.11 g/cm^3) is greater than the graphically calculated (0.98 g/cm^3). That concurs with the proposition that acid/base neutralization damages the support observed in FESEM results. Such aggressive protocol dissolves part of the support and penetrates it.
Double layer Nafion® membrane (T12) looks smooth and even in Figure 3.5. However, its thickness is quite an upsetting result. Membrane preparation protocol of T12 is simple inner coating with layering described in Chapter 2.1.2. Knowing that the 10% (w/w) aqueous solution has a density of approximately 1.05 g/cm^3, similar values should be calculated both from the weight gain and from the SEM results. Effectively, estimated density from weight gain is triple fold (3.52 g/cm^3) and graphically estimated density is even higher (5.56 g/cm^3).
Due to its weight loss between layers, it was suspected that every layer washed out the pre-existing one. Nevertheless, SEM results indicate the opposite phenomenon: every layer of the polymer adds up to the membrane and at the same time the aqueous solvent elutes, i.e., the weight change is produced by water loss.

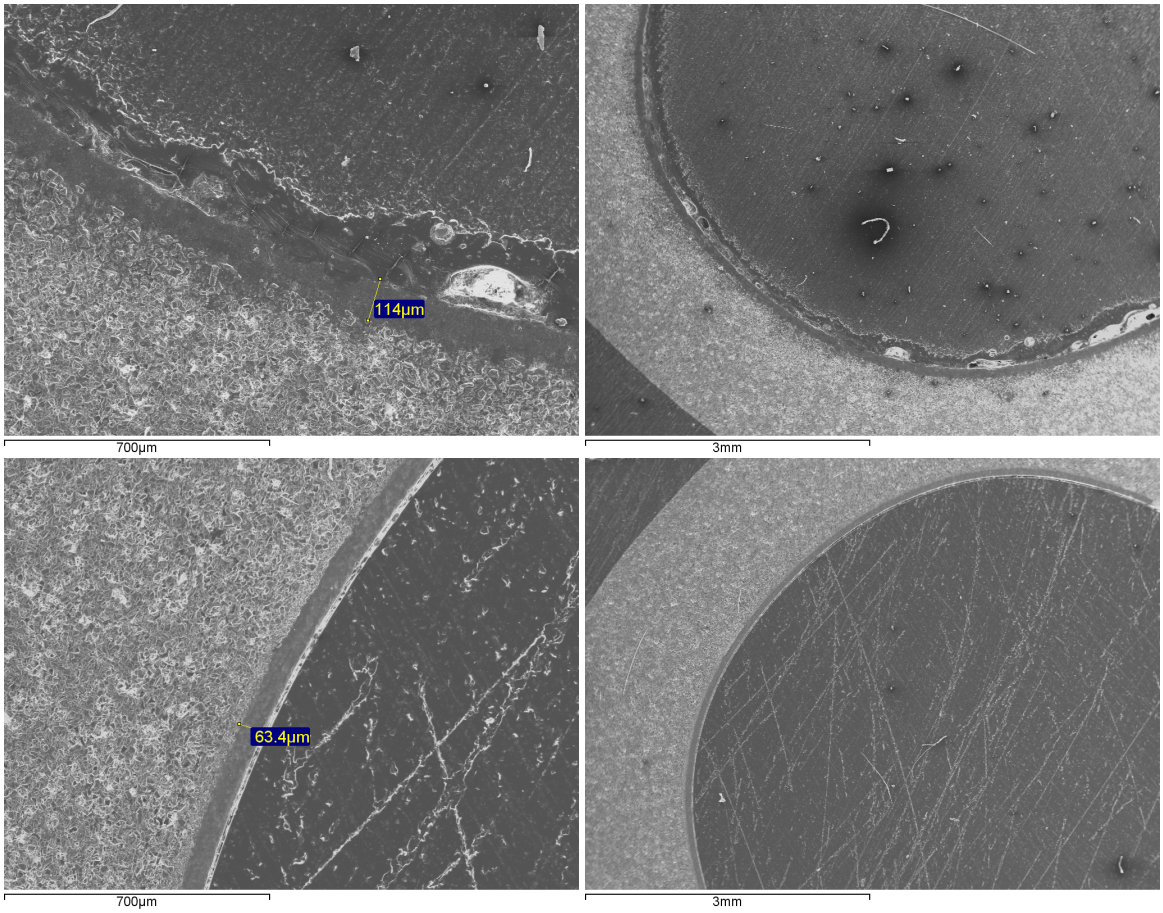

Figure 3.5: SEM results for Nafion® membranes. Upper row: T11; Bottom row: T12.

3.3 Gas separation assays: selectivities and permeance inside the reactor

Selectivities and separation factors are two calculated parameters which equations are shown in C.2. They are useful for membrane characterization because it is easy to measure whether a membrane is selective to certain molecules. Selectivity and separation factors are usually close values. In order to make a clear analysis and discussion of the results, only selectivity will be plotted. A positive result would be a membrane with high H_2O/H_2 and H_2O/CO_2 selectivities, indicating that the membrane is efficient at removing H_2O to a greater extent that the reactants permeate. H_2/CO_2 selectivity is also interesting because it tell the proportion which the reactants are permeating.
Furthermore, gas permeation measurements will help to infer the flow mechanism that is taking place. If the permeation proportion between H_2 and CO_2 is less than 4.69 (Equation 3.1), the flow mechanism will be pure Knudsen flow. As pressure increases, laminar flow starts to reign the flow mechanism because the gases permeate through the defects of the membrane. With greater laminar flow, the membrane loses its selectivity and the flow composition of the permeate streamline begins to be ever more similar to the feeding stream.

$$4.69 = \sqrt{\frac{M_{CO_2}}{M_{H_2}}} > \frac{Perm_{H_2}}{Perm_{CO_2}} \tag{3.1}$$

Additional phenomena such as H_2O flow or temperature influence in selectivity and integrity of the membranes are harder to predict. Some polymers swell with higher temperatures, others detach from the support with overpressure, others change their structure (hence selectivity and pore size) at certain temperatures, etc.
Anecdotally, sweeping gases also provided valuable information. Firstly, Ar would discreetly permeate in every experiment, so adjustments in the data processing were needed. Secondly, N_2 proved to be not necessary as sweeping carrier gas, facilitating the experimental design for future gas separation assays.

3.3.1 Silicone membranes

Figure 3.6 shows that, in all cases, H_2 permeance was higher than N_2 or CO_2 permeance, being the ratio similar to that predicted by Knudsen flow, i.e. the square root of the molecular weight ratio (Equation 3.1). Conversely, H_2O permeance was similar to H_2 permeance (excepting T5 at 0.02 H_2O mL/min) for the single layer membranes (T9 and T5) and even higher in the double layer membrane (T1), in spite of the much smaller molecular weight of H_2. This result implies that an additional mechanism for H_2O permeation is operating. Probably a solution-diffusion mechanism is acting in the case of H_2O permeation.
Double layer membrane had a much lower permeance for permanent gases (typically one order of magnitude smaller), while H_2O permeance was only decreased two fold in some cases. Therefore, a much higher H_2O/H_2 and H_2O/CO_2 selectivity is achieved with the double layer membrane, denoting that double layer membranes have fewer defects.
The results are clearer by looking to the H_2O/H_2 and H_2O/CO_2 selectivities in Figure 3.7. Both selectivities increase with temperature in the studied interval, which is an interesting result for the use of the silicone membranes. In particular, it seems that this kind of membranes would resist higher temperatures than the Nafion® membranes employed in previous work [12], allowing its use at temperatures more suitable to achieve a reasonable reaction rate with conventional catalysts.
H_2O/CO_2 selectivity is between 2 and 2.5 times greater than H_2O/H_2 selectivity, which matches with the hypothesis that a large part of both CO_2 and H_2 is permeating through small pores, corresponding to Knudsen flow. However, since that ratio was smaller than 4.69 some contribution of convective flow may exist.
The effect of H_2O partial pressure was different in each membrane. In the single layer membranes, an increase in H_2O partial pressure causes either a decrease(T9) or increase(T5) in H_2O permeance, i.e. the flux of H_2O did not increase linearly with the partial pressure of H_2O , indicating that H_2O solubility has a maximum value, like in a Langmuir adsorption isotherm. Meanwhile, the double layer membrane(T1) reached a maximum permeance at an intermediate partial pressure of H_2O .

The effect of temperature on the permeance of permanent gases was small. For the single layer membranes(T9 and T5), N_2 permeance decreased slightly with temperature, as may be expected for

Knudsen flow (Equation C.6), while H_2 permeance slightly increased, which suggest that H_2 permeation has a contribution from activated flow, i.e. pores with a size similar to that of the permeating molecule.

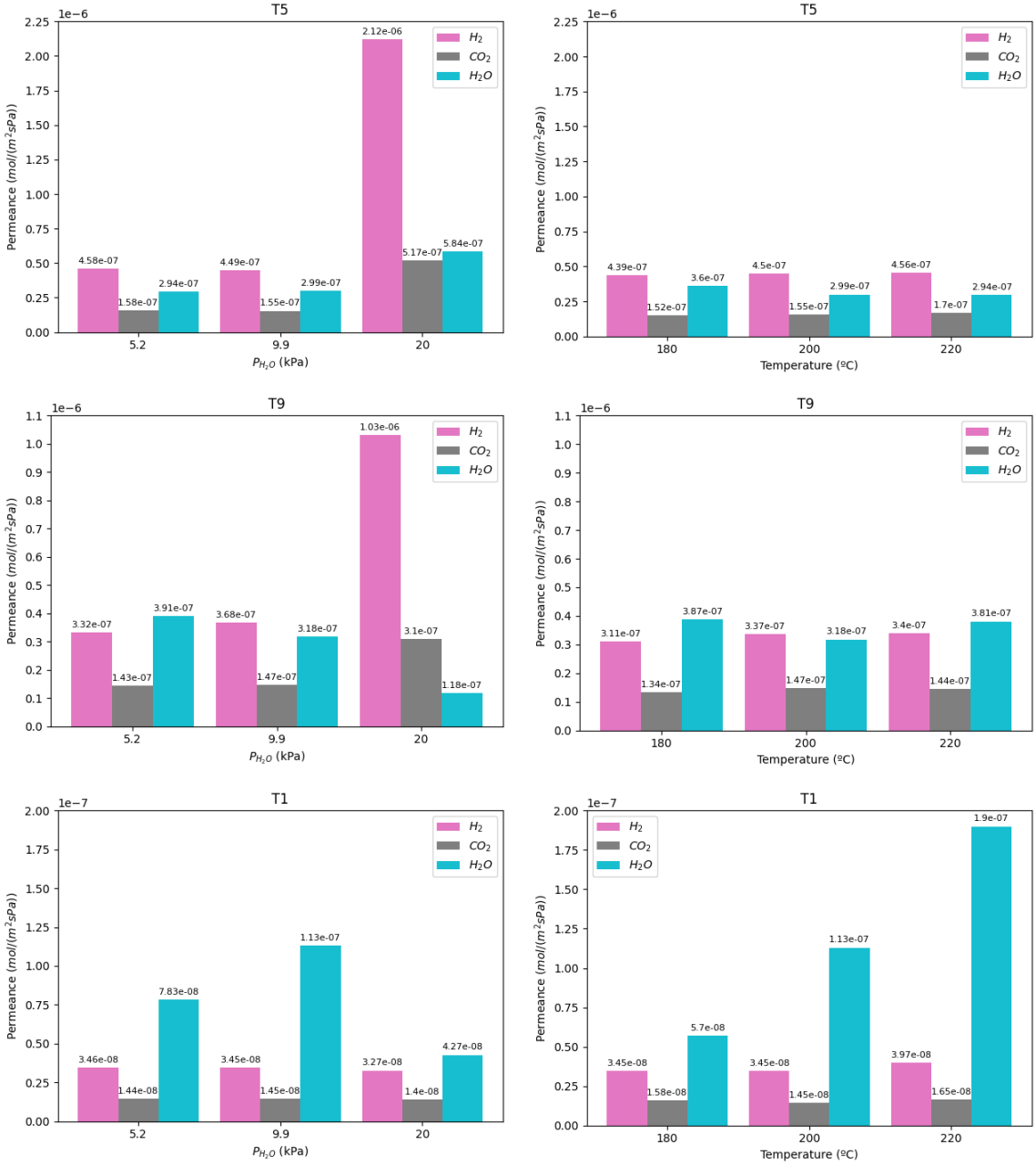

Figure 3.6: Gas separation permeance results in silicone membranes.

For the double layer membrane (T1), H_2 permeance decreased with temperature, which suggest that the diffusion through micropores was less significant than in the case of single layer membranes. The comparison of these membranes with previous results with zeolite membranes shows that the selectivity is a bit smaller. As an example, H_2O/H_2 selectivity with a zeolite membrane at 220ºC

was ca. 20 [21], while the result obtained with the double layer silicone membrane in this work was only 5. However, H_2O flux (2.5 $mmol/(m^2 * s)$) was similar to the one obtained with the zeolite membrane. The capability to achieve such flux is interesting, since the silicone-ceramic composite membrane can still be optimized, and thus could be competitive with the zeolite membrane.

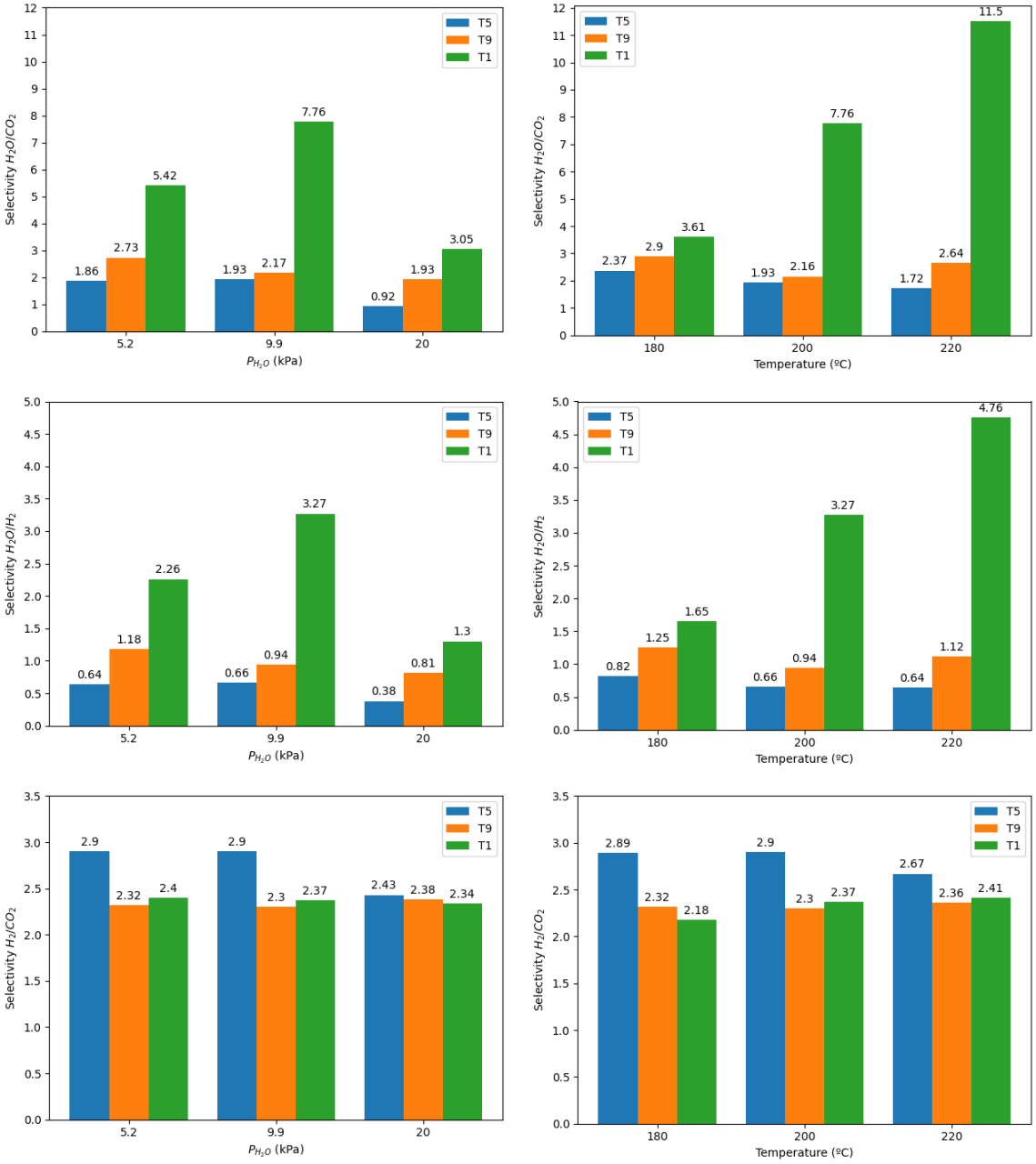

Figure 3.7: Calculated parameters from gas separation results in silicone membranes, at different conditions.

3.3.2 Nafion® membranes

Overall, Nafion® membranes results were not as promising as the silicone ones. In every condition tested, CO_2 permeance did not change with increasing H_2O partial pressures or higher temperatures, even though the polymer starts to degrade at 200ºC.
Total permeance was similar in both membranes. Also, the two membranes presented higher H_2O permeance with increase of H_2O partial pressures. H_2/CO_2 permeance ratios remained below 4.69 in every condition, but closer to this value than to 1. Therefore, the flow is closer to Knudsen flow than convective flow.
The effect of temperature raise was more noticeable for the triple layer membrane (T10), with a clear linear increase in H_2. Both membranes showed a more subtle increase in H_2O permeance. These observations highlight the fragile nature of Nafion®: as temperature raised, more defects allowed the gases to diffuse.

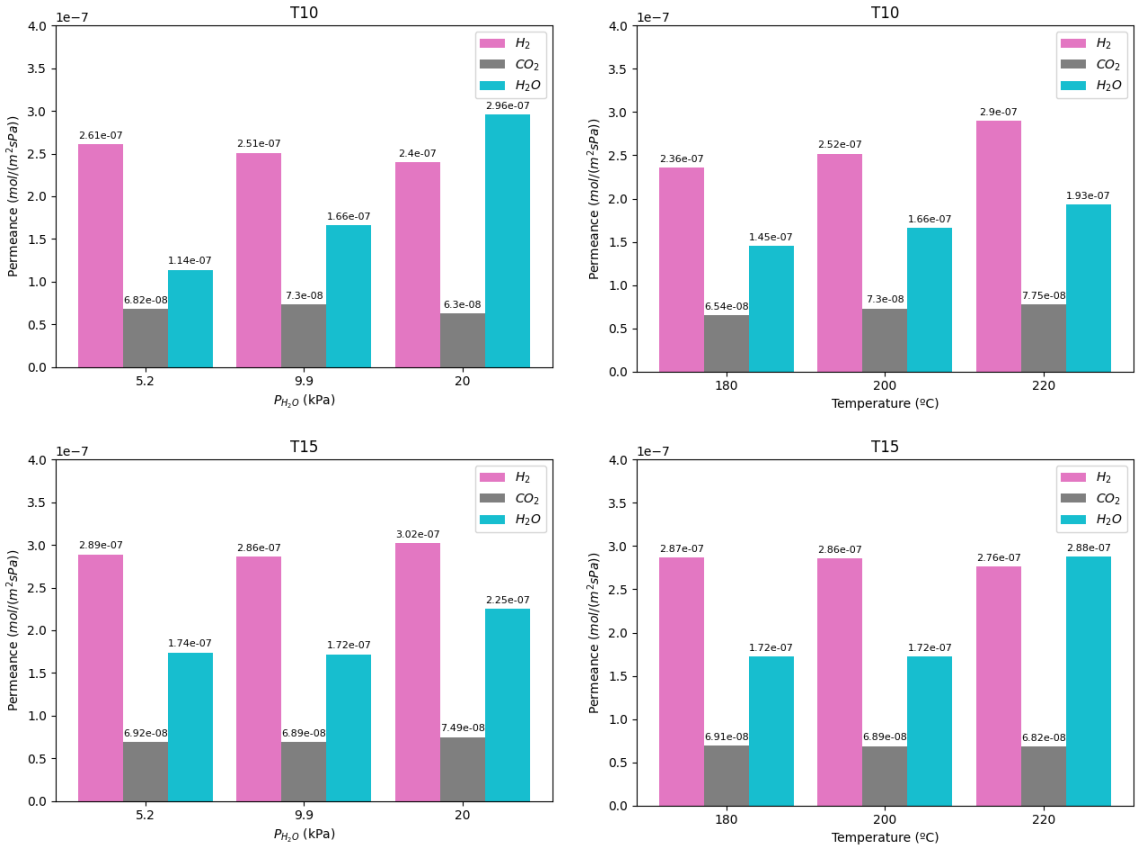

Figure 3.8: Gas separation permeance results in Nafion® membranes.

Regarding the three selectivities studied, H_2O/CO_2 selectivities consistently escalated as H_2O partial pressure or temperature increased (Figure 3.9). The values were not extraordinarily high, but still positive results that suggested a better performance of the membranes close to reaction conditions. H_2O/H_2 and H_2/CO_2 selectivities did not change significantly at different conditions, and both of them cued the conclusion that the defects in Nafion® were too large and abundant for the membranes to be selective. On one side, low H_2O/H_2 selectivity indicated that H_2 permeated at a

higher rate than H_2O. On the other side, high H_2/CO_2 selectivity led to the same point: H_2 was a small molecule that could easily pass through Nafion® pores.

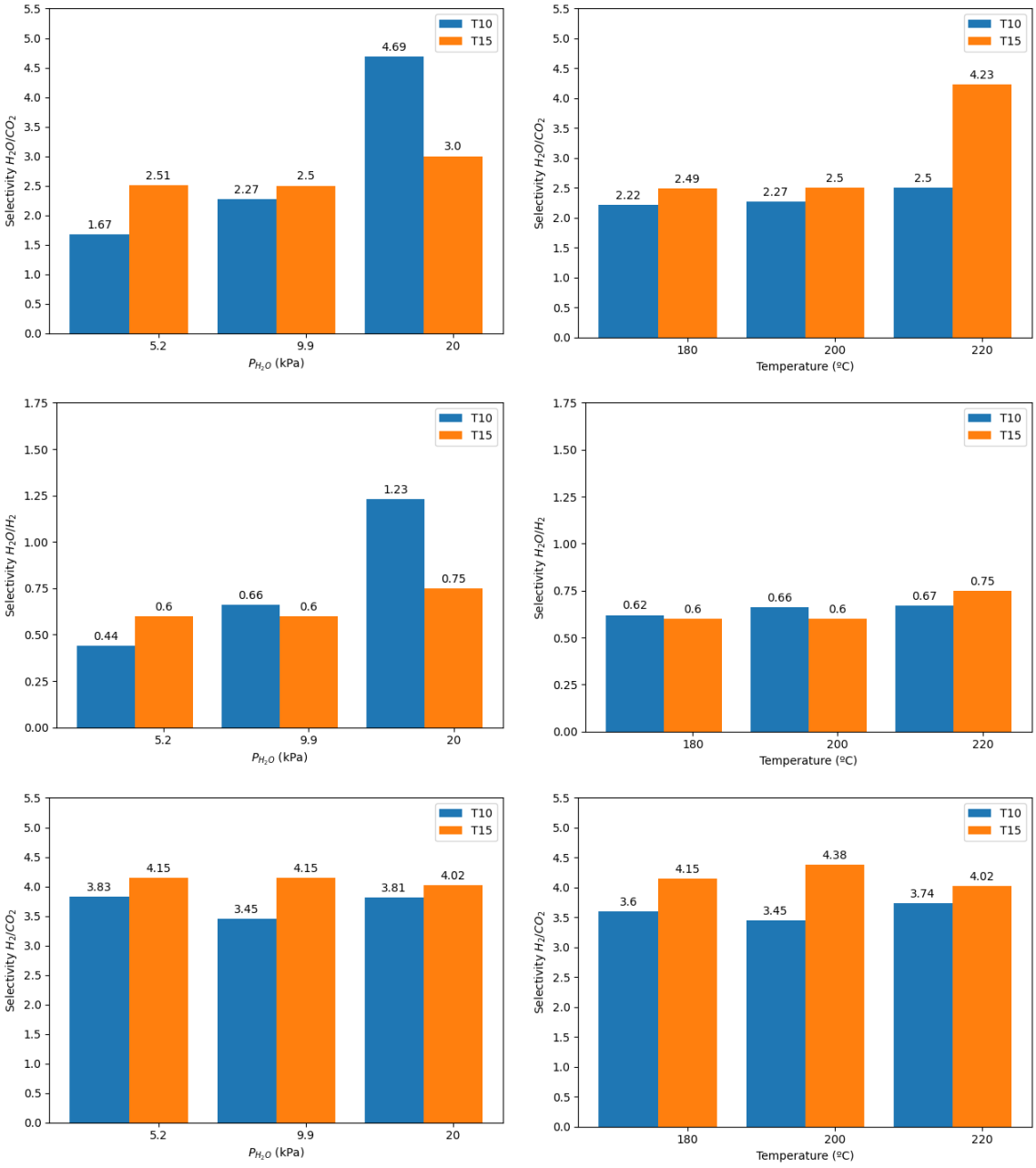

Figure 3.9: Calculated parameters from gas separation results in Nafion® membranes, at different conditions.

H_2O/H_2 selectivity was intermediate between the values corresponding to Knudsen flow (0,33) and convective flow (1). This result suggests that, contrarily to the results in silicone membranes, the contribution from a diffusion-solution mechanism (that would contribute to the selective flow of water) is negligible.

Chapter 4

Conclusions and future work

Silicone rubber membranes deposited on ceramic supports can remove selectively H_2O from a mixture of gases containing H_2 and CO_2 at temperatures up to 220ºC. Therefore, they may be useful for membrane reactors that synthesize methanol by CO_2 hydrogenation. The best obtained H_2O/H_2 selectivity was 4.8 at 220ºC, with a H_2O permeance of $1.40 * 10^{-7} \frac{mol}{m^2 s Pa}$. N_2 permeation suggests the presence of small pores (defects) that decrease H_2O/H_2 selectivity. Further optimization of the preparation procedure should be needed to achieve a membrane with comparable selectivity to that obtained with zeolite membranes, but if such polymer-ceramic membranes were achieved, they could have many applications in membrane reactors for processes where the removal of water improves the achievable yield [27] [28]. Technical difficulties in Nafion® membranes preparation and inconsistent results led to discontinue its development.

We are proud to announce that a paper has been published about this project [29] and the research is being continued by new students at the *Chemical Engineering and Environmental technologies Department* in the *Engineering Research Institute of Aragon (I3A)*.

Appendix A

European Comission recent related projects

European Comission research projects from 2015 to 2020 resulting from cross-referencing 'methanol' and 'hydrogenation'.
Source: CORDIS data repository (https://cordis.europa.eu/en)

- FReSMe
- CuZnSyn
- MONACAT
- CIRCLENERGY
- CASCADE-X
- Djewels
- COUPC1
- PROMET-H2
- HyMethShip
- OPERANDOCAT
- NTPleasure
- LOTER.CO2M
- COFLeaf
- ZEOSEP

Appendix B

Silicone membranes preparation protocol

Reactants:

- RTV-801 Silicone
- DBTL catalyst ($d_{cat} = 1.05 g/ml$)
- Fractional hexane ($d_{hex} = 0.672 g/ml$)

Constant weighing provides information about any polymer loss during the pipetting or calcination steps. Starting with a calcined enamelled tubular ceramic membrane (Figure B.1), which weight is known:

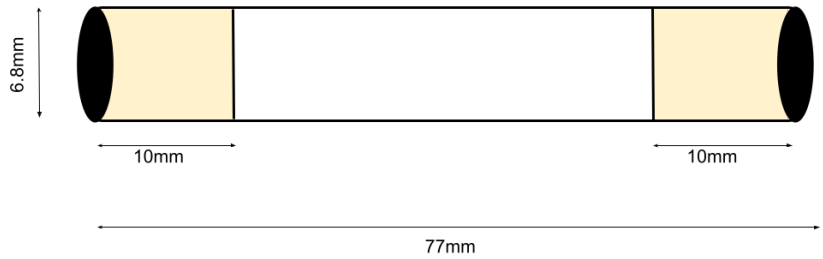

Figure B.1: Measurements of an enamelled tubular ceramic membrane.

1. Weigh the desired amount of silicone directly adhered to the glass rod that is going to be used to stir the solution. For a X_i mass proportion expressed in times one of silicone, $m_i(g)$ mass can be calculated as

$$m_i = \frac{X_i * d_{hex} * V_{hex}}{1 - X_i}$$

2. Dissolve the silicone without letting it touch the recipient walls.
3. Add $100 \mu L$ of DBTL to the solution.
   (a) **Light membrane** option: carefully pipette the entire solution 5-10 times through the inner wall of the ceramic membrane. Try to cover all the inner surface. Let it dry at room temperature and weigh.
   (b) **Heavy membrane** option: plug one of the ceramic membrane extremes and add enough solution to cover all the inner wall. Let it sit for 5min. Plug the other side, turn around

and unplug the first side. Let it sit another 5min. Repeat until the hexane has evaporated (the ceramic will be at room temperature again). Weigh.

4. Calcination is optional. Temperature ramp is 2ºC/min until reaching 350ºC, stay 3h at 350ºC and ramp up to 500ºC at 2ºC/min, stay 4h. Weigh again.

5. Pipette fractional hexane over the flaked silicone until there is a smooth layer left. Let it dry at room temperature and weigh again.

Appendix C

Formulas and models

C.1 Flows

$$Volumetric\ flow = \frac{\overline{x_i}}{t} \quad [\frac{mL}{s}] \tag{C.1}$$

$$Molar\ flow = \frac{p\ \overline{x_i}\ 0.001}{R\ T\ t} \quad [\frac{mol}{s}] \tag{C.2}$$

$$Permeance = \frac{p\ \overline{x_i}\ 0.001}{R\ T\ t\ p^*\ 2\pi\ r\ h} \quad [\frac{mol}{s\ m^2\ Pa}] \tag{C.3}$$

$$Laminar\ flow\ (empirical) = \frac{\epsilon\ r_{pore}^2}{8\ L\ \tau\ \mu\ R\ T} *\ p \quad [\frac{mol}{s\ m^2\ Pa}] \tag{C.4}$$

$$Knudsen\ flow\ (empirical) = \frac{4\ \epsilon\ r_{pore}}{3\ L\ \tau}\ \sqrt{\frac{2}{\pi\ M\ R\ T}} \quad [\frac{mol}{s\ m^2\ Pa}] \tag{C.5}$$

$$Total\ permeance\ (empirical) = Laminar\ flow\ +\ Knudsenflow \tag{C.6}$$

C.2 Calculated parameters

$$Selectivity_{\frac{a}{b}} = \frac{\chi_{perm,a}\ \Delta P_b}{\chi_{perm,b}\ \Delta P_a} \tag{C.7}$$

$$Separationfactor_{\frac{a}{b}} = \frac{\chi_{ret,b}\ \chi_{perm,a}}{\chi_{ret,a}\ \chi_{perm,b}} \tag{C.8}$$

$$Logarithmic\ mean_a = \frac{(\chi_{a,in}^{ret} - \chi_{a,in}^{perm}) - (\chi_{a,out}^{ret} - \chi_{a,out}^{perm})}{\ln \frac{\chi_{a,in}^{ret} - \chi_{a,in}^{perm}}{\chi_{a,out}^{ret} - \chi_{a,out}^{perm}}} \quad [bar] \tag{C.9}$$

Bibliography

[1] "Global Energy & CO2 Status Report 2018". In: International Energy Agency, Paris, France, 2019.

[2] "World Energy Outlook". In: International Energy Agency, Paris, France, 2018.

[3] "Early Estimates of CO2 Emissions from Energy Use". In: News Release, Eurostat, Brussels, Belgium, 2014.

[4] G. A. Olah. "Beyond oil and gas: The methanol economy". In: *Angewandte Chemie - International Edition* 44.18 (2005), pp. 2636–2639. ISSN: 14337851. DOI: 10.1002/anie.200462121.

[5] A. Goeppert, M. Czaun, J. P. Jones, G. K. Surya Prakash, and G. A. Olah. "Recycling of carbon dioxide to methanol and derived products-closing the loop". In: *Chemical Society Reviews* 43.23 (2014), pp. 7995–8048. ISSN: 14604744. DOI: 10.1039/c4cs00122b.

[6] S. S. Araya, V. Liso, X. Cui, N. Li, J. Zhu, S. L. Sahlin, S. H. Jensen, M. P. Nielsen, and S. K. Kær. "A review of the methanol economy: The fuel cell route". In: *Energies* 13.3 (2020). ISSN: 19961073. DOI: 10.3390/en13030596.

[7] G. A. Olah. "Towards oil independence through renewable methanol chemistry". In: *Angewandte Chemie - International Edition* 52.1 (2013), pp. 104–107. ISSN: 14337851. DOI: 10.1002/anie.201204995.

[8] A. Wójcik. "Haldor Topsoe joins ambitious sustainable fuel project in Denmark". In: 2020. URL: topsoe.com.

[9] "Carbon Recycling International". In: 2020. URL: https://www.carbonrecycling.is/news-media/fresmemilestone.

[10] A. Stankiewicz. "Reactive separations for process intensification: An industrial perspective". In: *Chemical Engineering and Processing* 42.3 (2003), pp. 137–144. ISSN: 02552701. DOI: 10.1016/S0255-2701(02)00084-3.

[11] R. Guil-López, N. Mota, J. Llorente, E. Millán, B. Pawelec, J. L. Fierro, and R. M. Navarro. "Methanol synthesis from CO2: A review of the latest developments in heterogeneous catalysis". In: *Materials* 12.23 (2019). ISSN: 19961944. DOI: 10.3390/ma122333902.

[12] R. P. Struis, S. Stucki, and M. Wiedorn. "A membrane reactor for methanol synthesis". In: *Journal of Membrane Science* 113.1 (1996), pp. 93–100. ISSN: 03767388. DOI: 10.1016/0376-7388(95)00222-7.

[13] G. Barbieri, G. Marigliano, G. Golemme, and E. Drioli. "Simulation of CO2 hydrogenation with CH3OH removal in a zeolite membrane reactor". In: *Chemical Engineering Journal* 85 (2002), pp. 53–59.

[14] G. Liu, W. Wei, W. Jin, and N. Xu. "Polymer/ceramic composite membranes and their application in pervaporation process". In: *Chinese Journal of Chemical Engineering* 20.1 (2012), pp. 62–70.

ISSN: 10049541. DOI: 10.1016/S1004-9541(12)60364-4. URL: http://dx.doi.org/10.1016/S1004-9541(12)60364-4.

[15] M. Menéndez Sastre, E. Piera, J. Coronas Ceresuela, and J. Santamaría Ramiro. "Reactor de membrana zeolítica para la obtención de metanol y otros alcoholes a partir de gas de síntesis". In: Spain Patent 2 164 544 B1, May, 2003.

[16] F. Gallucci, L. Paturzo, and A. Basile. "An experimental study of CO2 hydrogenation into methanol involving a zeolite membrane reactor". In: *Chemical Engineering and Processing: Process Intensification* 43.8 (2004), pp. 1029–1036. ISSN: 02552701. DOI: 10.1016/j.cep.2003.10.005.

[17] H. Li, C. Qiu, S. Ren, Q. Dong, S. Zhang, F. Zhou, X. Liang, J. Wang, S. Li, and M. Yu. "Na+-gated water-conducting nanochannels for boosting CO2 conversion to liquid fuels". In: *Science* 367.6478 (2020), pp. 667–671. ISSN: 10959203. DOI: 10.1126/science.aaz6053.

[18] P. Shao and R. Y. Huang. "Polymeric membrane pervaporation". In: *Journal of Membrane Science* 287.2 (2007), pp. 162–179. ISSN: 03767388. DOI: 10.1016/j.memsci.2006.10.043.

[19] X. Feng, P. Shao, R. Y. Huang, G. Jiang, and R. X. Xu. "A study of silicone rubber/polysulfone composite membranes: Correlating H2/N2 and O2/N2 permselectivities". In: *Separation and Purification Technology* 27.3 (2002), pp. 211–223. ISSN: 13835866. DOI: 10.1016/S1383-5866(01)00196-4.

[20] P. Poletto, D. da Silva Biron, M. Zeni, C. P. Bergmann, and V. dos Santos. "Preparation and characterization of composite membranes ceramic/PSf and ceramic/PA 66". In: *Desalination and Water Treatment* 51.13-15 (2013), pp. 2666–2671. ISSN: 19443986. DOI: 10.1080/19443994.2012.749308.

[21] J. Gorbe, J. Lasobras, E. Francés, J. Herguido, M. Menéndez, I. Kumakiri, and H. Kita. "Preliminary study on the feasibility of using a zeolite A membrane in a membrane reactor for methanol production". In: *Separation and Purification Technology* 200 (2018), pp. 164–168. ISSN: 18733794. DOI: 10.1016/j.seppur.2018.02.036. URL: https://doi.org/10.1016/j.seppur.2018.02.036.

[22] B. Libby, W. H. Smyrl, and E. L. Cussler. "Polymer-zeolite composite membranes for direct methanol fuel cells". In: *AIChE Journal* 49.4 (2003), pp. 991–1001. ISSN: 00011541. DOI: 10.1002/aic.690490416.

[23] G. Chen and Q. Yuan. "Methanol synthesis from CO2 using a silicone rubber/ceramic composite membrane reactor". In: *Separation and Purification Technology* 34.1-3 (2004), pp. 227–237. ISSN: 13835866. DOI: 10.1016/S1383-5866(03)00195-3.

[24] S. Ren, G. Sun, C. Li, Z. Liang, Z. Wu, W. Jin, X. Qin, and X. Yang. "Organic silica/Nafion® composite membrane for direct methanol fuel cells". In: *Journal of Membrane Science* 282.1-2 (2006), pp. 450–455. ISSN: 03767388. DOI: 10.1016/j.memsci.2006.05.050.

[25] Z. Siroma, N. Fujiwara, T. Ioroi, S. Yamazaki, K. Yasuda, and Y. Miyazaki. "Dissolution of Nafion® membrane and recast Nafion® film in mixtures of methanol and water". In: *Journal of Power Sources* 126.1-2 (2004), pp. 41–45. ISSN: 03787753. DOI: 10.1016/j.jpowsour.2003.08.024.

[26] T. Mohammadi, A. Aroujalian, and A. Bakhshi. "Pervaporation of dilute alcoholic mixtures using PDMS membrane". In: *Chemical Engineering Science* 60.7 (2005), pp. 1875–1880. ISSN: 00092509. DOI: 10.1016/j.ces.2004.11.039.

[27] M. Menéndez. “Inorganic Membrane Reactors for Energy Applications”. In: Sept. 2011, pp. 283–297. ISBN: 978-981-4267-17-5. DOI: 10.1201/b11168-14.

[28] N. Diban, A. T. Aguayo, J. Bilbao, A. Urtiaga, and I. Ortiz. “Membrane Reactors for in Situ Water Removal: A Review of Applications”. In: *Industrial & Engineering Chemistry Research* 52.31 (2013), pp. 10342–10354. DOI: 10.1021/ie3029625.

[29] E. Juarez, J. Lasobras, J. Soler, J. Herguido, M. Menéndez, and M. A. Soria. “membranes Polymer-Ceramic Composite Membranes for Water Removal in Membrane Reactors”. In: (2021). DOI: 10.3390/membranes11070472.